Protein Engineering vol.11 no.6 pp.447–455, 1998

Probing the stabilizing role of C-terminal residues in trimethylamine dehydrogenase

O.W.D.Ertughrul, N.Errington, S.Raza[1], M.J.Sutcliffe[1], A.J.Rowe and N.S.Scrutton[2]

Departments of Biochemistry and [1]Chemistry, University of Leicester, Adrian Building, University Road, Leicester LE1 7RH, UK

[2]To whom correspondence should be addressed

In trimethylamine dehydrogenase, a homodimeric iron–sulfur flavoprotein, the C-terminal 17 residues of each subunit (residues 713–729) embrace residues on the other subunit. The role of this unusual mode of interaction at the subunit interface was probed by isolating three mutant forms of trimethylamine dehydrogenase in which the C-terminus of the enzyme was deleted by five residues [Δ(725–729), 10 residues [Δ(720–729)] and 17 residues [Δ(713–729)]. The solution properties and conformational states of the three mutant enzymes were investigated using optical, fluorescence and circular dichroism spectroscopies, ANS binding and a novel and conformationally sensitive hydrodynamic method. The data reveal that sequential deletion of the C-terminus of trimethylamine dehydrogenase does not affect significantly dimer stability or the overall structural integrity of the enzyme. However, deletion of the C-terminus severely compromises, but does not abolish, the ability of the enzyme to become covalently coupled with the redox cofactor FMN in the active site, located over 20 Å from the C-terminus. Hydrodynamic studies reveal minor conformational changes in the deletion mutants that lead to a more compact enzyme structure. These conformational changes are probably transmitted to the active site via altering the interaction of the C-terminus with the second helix in the β/α barrel of trimethylamine dehydrogenase, leading to poor flavinylation during the folding of the enzyme and assembly with FMN.

Keywords: trimethylamine dehydrogenase/hydrodynamics/C-terminal deletions/flavoprotein

Introduction

Trimethylamine dehydrogenase (TMADH; EC 1.5.99.7) is a homodimeric, multi-domain iron–sulfur flavoprotein found in a variety of methylotrophic bacteria. Its function is to catalyse the oxidative demethylation of trimethylamine to form dimethylamine and single-carbon units in the form of formaldehyde for anabolism (Steenkamp and Mallinson, 1976).

$$(CH_3)_3N + H_2O \rightarrow (CH_3)_2NH + CH_2O + 2H^+ + 2e^-$$

The enzyme from *Methylophilus methylotrophus* (sp. W_3A_1) is a homodimer, each subunit containing a 4Fe–4S centre (Hill *et al*., 1977), a 6-*S*-cysteinyl FMN (Kenney *et al*., 1978; Steenkamp *et al*., 1978a,b) and ADP (Lim *et al*., 1988). The function of the latter cofactor is unknown, but it may represent the vestigial remains of an ancestral dinucleotide-binding domain (Lim *et al*., 1988; Scrutton, 1994). The crystal structure of the enzyme is known at 2.4 Å resolution (Lim *et al*., 1986; Brookhaven code 2TMD) and has recently been refined at 1.8 Å resolution (F.S.Mathews *et al*., unpublished). The availability of the crystal structure has enabled detailed investigations of the catalytic mechanism. Kinetic studies of the reductive half-reaction (Rohlfs and Hille, 1994; Falzon and Davidson, 1996a; Basran *et al*., 1997) and internal electron transfer from the 6-*S*-cysteinyl FMN to the 4Fe–4S centre (Rohlfs and Hille, 1991; Rohlfs *et al* 1995; Falzon and Davidson, 1996b) have been described. In the oxidative half-reaction, electrons are passed individually in two sequential steps to the FAD of an electron transferring flavoprotein (ETF) (Steenkamp and Gallup, 1978). The kinetics of this process in wild-type (Huang *et al*., 1995) and mutant complexes (Wilson *et al*., 1997a), and studies of the molecular assembly of the TMADH·ETF electron transfer complex by equilibrium ultracentrifugation have been reported (Wilson *et al*., 1997b). The availability of the cloned gene encoding TMADH (Boyd *et al*., 1992) has enabled studies of the flavinylation mechanism of the enzyme by site-directed mutagenesis (Scrutton *et al*., 1994), mass spectrometry (Packman *et al*., 1995; Mewies *et al*., 1996) and X-ray crystallography (Mathews *et al*., 1996). The X-ray structure of trimethylamine dehydrogenase reveals three domains per subunit; an N-terminal β/α barrel domain that contains the active site 6-*S*-cysteinyl FMN, a medium domain and a small domain (Lim *et al*., 1986). The ADP molecule binds to the medium domain (Lim *et al*., 1988) and the 4Fe–4S centre is located in a small peptide loop buried at the junction of the β/α barrel and the medium domain. The interaction site for ETF has been mapped to a surface concavity centred around residue Tyr442 (Wilson *et al*., 1997a), and its location is consistent with the formation of binary and/or ternary electron transfer complexes (Wilson *et al*., 1997b).

The interface between the two subunits of TMADH is extensive (approximately 6100 $Å^2$), which accounts for the lack of dissociative behaviour in solution (Cölfen *et al*., 1996). Interestingly, the C-terminal 17 residues of each subunit (residues 713–729) wrap around surface residues on the other subunit. This observation suggests that their role may be (i) to confer stability on the assembled homodimer by embracing surface residues on the other subunit, and/or (ii) to guide dimer formation during subunit–subunit association. To probe the role of the C-terminal 17 residues of TMADH, we have studied wild-type enzyme (where residue 729 is at the C-terminus) and three mutant forms [Δ(725–729), Δ(720–729) and Δ(713–729)], deleted in the C-terminal region by 5, 10 and 17 residues, respectively. Their conformational states and solution properties have been characterized using optical, fluorescence emission and circular dichroism spectroscopies, ANS binding and a novel, sensitive, analytical ultracentrifugation technique.

Materials and methods

Materials

Complex bacteriological media was prepared as described by Sambrook *et al.* (1989) using materials purchased from Unipath

Ltd. *Escherichia coli* strain JM109 [rk$^-$, mk$^+$, *rec*A1, *sup*E, *end*A1, *hsd*R17, *gyr*A96, *rel*A1, *thi*, Δ(*lac-pro* AB) F′ *tra*D36, *pro*A$^+$B$^+$, *lac*I^q, *lac*ZΔM15] was from Stratagene. Restriction enzymes and Vent DNA polymerase were purchased from Pharmacia Biotech Inc. Calf intestinal alkaline phosphatase was from Boehringer Mannheim. T4 DNA ligase was from Promega; T4 polynucleotide kinase was obtained from Amersham International. Timentin was from Beecham Research Laboratories. Ascorbic acid, riboflavin, 3-(2-pyridyl)-5,6-bis(4-phenylsulfonic acid)-1,2,4-triazine (ferrozine), 8 anilino-1-naphthalene sulfonic acid (ANS), trimethylamine (HCl salt), phenozine methosulfate (PMS) and dichlorophenolindophenol (DCPIP) were from Sigma. All other chemicals were of analytical quality where possible. Water was glass-distilled and further purified by the Elgastat UHP System.

Mutagenesis, plasmid construction and DNA sequencing

Plasmid DNA and bacteriophage replicative-form DNA were prepared using Promega Maxi and Mini kits. Miniscale single-stranded bacteriophage DNA was prepared as described elsewhere (Sambrook *et al*., 1989). Restriction endonuclease digestion and ligation of DNA were carried out as recommended by the enzyme suppliers. Site-directed mutagenesis was carried out on the coding strand of the *tmd* gene contained within the M13-based construct M13TM3 (Scrutton *et al*., 1994), using the phosphorothioate method marketed by Amersham International. Overexpression and purification of recombinant proteins was performed as described for recombinant wild-type and other mutant forms of TMADH (Scrutton *et al*., 1994). Opal and ochre stop codons were introduced at residue positions 713 and 720, respectively, by site-directed mutagensis using the oligonucleotides 5′-ATATGCGGCGTGCCTCATGCGATGGTTTCA-3′ [TMADH Δ(713–729)] and 5′-ATTTTGAAATTACCTTATGGCATATGCGGC-3′ [TMADH Δ(720–729)]. Expression constructs were generated by replacement of the 0.8 kb *Hin*dIII fragment found within the wild-type *tmd* gene of plasmid pSV2tmdveg (Scrutton *et al*., 1994) with the analogous fragment released from the mutant bacteriophage by digestion with *Hin*dIII. The entire 0.8 kb *Hin*dIII fragment containing the desired mutagenic change was resequenced to ensure no spurious mutations arose during the mutagenesis reactions. An ochre stop codon at residue 725 was introduced by the polymerase chain reaction using M13TM3 bacteriophage RF DNA as template (Scrutton *et al*., 1994). The C-terminal oligonucleotide 5′-TTTTTTTTTAAGCTTGTACTCTTATTTGAAATTACC-3′ was designed to contain the ochre codon and a *Hin*dIII site downstream of the codon. The N-terminal oligonucleotide 5′-GATGGAAAGCGGTTATAC-3′ was designed to bind upstream of a unique *Hin*dIII site within the *tmd* gene (Boyd *et al*., 1992). Conditions used in PCR amplification were 2 min at 95°C (denaturation), 1 min at 48°C (annealing) and 1 min at 72°C (extension). The amplified fragment of 957 bp was subsequently digested with *Hin*dIII and used to replace the corresponding fragment released from plasmid pSV2tmdveg by digestion with *Hin*dIII. Again, the introduced fragment was completely re-sequenced to ensure no spurious mutations arose during the amplification process.

Protein expression and purification

Native TMADH was purified from *Methylophilus methylotrophus* (sp W3A1) as previously described (Wilson *et al*., 1995). *Escherichia coli* strain JM109 transformed with the wild-type and mutant expression plasmids were cultured in 2×YT media, supplemented with 100 mg/l timentin, 100 mg/l riboflavin and 200 mg/l iron (II) sulfate. Mutant proteins were expressed constitutively under the control of the *Bacillus subtilis veg* promoter into late stationary phase. Cells were harvested and the mutant protein purified as described previously for the wild-type protein (Scrutton *et al*., 1994). Enzyme purity was assessed by SDS–PAGE (Laemmli, 1974) in homogeneous (15%) gels and stained with Coomassie brilliant blue R250. Protein concentration was determined by either UV spectroscopy, the Bradford protein assay (Bradford, 1976) or visible spectroscopy using the known extinction of native TMADH subunit (27 300 $M^{-1}cm^{-1}$; Kasprazak *et al*., 1983) and calculated extinctions of the mutant enzymes (see below).

Analytical procedures, fluorescence and circular dichroism spectroscopy

Each of the enzyme preparations were analysed for the presence of the three co-factors, ADP, FMN and 4Fe–4S centre, using spectrophotometric and fluorimetric assays described previously (Scrutton *et al*., 1994; Mewies *et al*., 1996). Circular dichroism spectroscopy was performed using a Jobin Yvon CD6 instrument. Far-UV data were collected at 20°C from 190–250 nm using an integration time of 1 s and three scans were performed per sample; protein concentration was 0.2 mg/ml and was contained in 50 mM potassium phosphate buffer, pH 7.6. Near-UV data were collected at 20°C from 250–310 nm using an integration time of 1 s and 10 scans were performed per sample; protein concentration was 1 mg/ml contained in 50 mM potassium phosphate buffer, pH 7.6. The pathlength for far- and near-UV data was 0.5 mm.

Fluoresence measurements were performed using a Sim Aminco fluorimeter with Xenon light source. Measurements were conducted at 20°C at a protein concentration of 0.2 or 0.1 mg/ml (for ANS binding experiments); samples were contained in 50 mM potassium phosphate buffer, pH 7.6. A stock solution of ANS was prepared in 50 mM potassium phosphate buffer, pH 7.5 and its concentration was determined at 350 nm using an extinction coefficient of 4950 $M^{-1}cm^{-1}$, according to the procedure described by Weber and Young (1964). ANS concentration in the cuvette was 25 μM, and fluorescence emission spectra were recorded at an excitation wavelength of 365 nm from 450 to 650 nm.

Wild-type and mutant enzymes were assayed under steady-state conditions using the artificial electron acceptor phenozine methosulfate and dichlorophenolindophenol as described previously (Basran *et al*., 1997). Assays were performed in 100 mM sodium pyrophosphate buffer, pH 8.5, at 30°C, in a final volume of 1 ml. For specific activity calculations, trimethylamine concentration was 100 μM. Steady-state kinetic parameters were calculated by non-linear least squares fitting to the appropriate rate equation (see below). Data fitting was performed using Kaleidograph software (Abelbeck Software). Units of enzyme activity are expressed as μmol of DCPIP reduced per minute.

Sedimentation velocity analysis

Samples at a concentration of 1.3 mg/ml were analysed in an MSE Mk II Analytical Ultracentrifuge fitted with Variable Geometry Laser Optics (Errington and Rowe, to be published) with emission at 543 nm, and an AUC Imager (Clelow *et al*., 1997) for data capture and analysis. The operating speed was 34 000 r.p.m., and the temperature was 20°C. For purposes of comparison of the frictional properties of the wild-type and

mutants, three samples were run concurrently in the rotor, multiplexed by use of ±2° wedge windows, with one channel being allocated to the native wild-type as the reference. Care was taken to ensure that the protein concentrations were identical in all channels.

Using phase-plate schlieren optics, images were logged automatically to disk in the control computer (Power PC 7100) every 20 min, as files in NIH-Image. After automatic subtraction of a common 'background' image (i.e. with the phase-plate removed) from all recorded images, traces recorded at times when the solvent baseline was near to symmetrical around the solute boundary region were analysed using the locally written program LINEDEF, and logged to disk as files of d*n*/d*r* versus *r*, where *n* is the refractive index and *r* the radial position from the centre of the rotor. After subtraction of a linear baseline, these files were transformed into files of the function g(*s**) versus *s* via the Bridgman equation [Bridgman, 1942; where *s* is the sedimentation coefficient and g(*s**) is the apparent distribution of *s* values with respect to *s*]. All these latter manipulations were performed within the application ProFit. The software set written for the AUC Imager and used in all these operations is described elsewhere (Clelow *et al*., 1997). The $g(s^*)_{max}$ value [i.e. the most frequent value of g(*s**)] was then estimated for each sample from the fitting of a single Gaussian function using standard procedures in ProFit.

The optics of the MSE Mk II Analytical Ultracentrifuge were aligned prior to use, by means of conventional methods (Lloyd, 1974). Particular care was taken to focus the camera lens initially onto the mid-plane of the 10 mm pathlength cells. For this purpose, the optics were initially aligned for multi-slit source Rayleigh interference optics, which are extremely stringent in their requirement for focussing of the camera lens on this plane. The camera lens was then relocated such that it was focussed onto the 2/3rds plane of the cell (from the inner side of the entrance window), using the vernier on the saddle on the Oriel precision optical bench. Finally, recorded schlieren velocity patterns, transformed into g(*s**) versus *s* distributions for known monodisperse standards, were checked for the absence of 'Wiener skewing' which arises from mal-focussing of the camera lens (Svensson, 1954; Lloyd, 1974). It was assumed that the second order 'aperture effect' (Svennson, 1954) was negligible, since the angular aperture in the plane normal to radial was very small indeed as a consequence of the schlieren slit being defined by a one-dimensional laser beam expander.

As a calibration standard for the absolute *s* value of wild-type TMADH, a sedimentation velocity run was perfomed on the sample in a Beckman Optima XL-A Analytical Ultracentrifuge, using absorption optics and scanning at 280 nm. The program SVEDBERG (J Philo) was employed for analysis. The accuracy of this determination is high (principally by virtue of the very good temperature control of the rotor), but the precision of absorption optics is inferior to that which can be obtained using refractometric optics, especially when g(*s**) profiles are employed. It should be noted that it is legitimate to compare $g(s^*)_{max}$ with a sedimentation coefficient determined from boundary migration provided that the former has been computed by a procedure free of approximations, as in the present case where the Bridgman equation (Bridgman, 1942) has been employed.

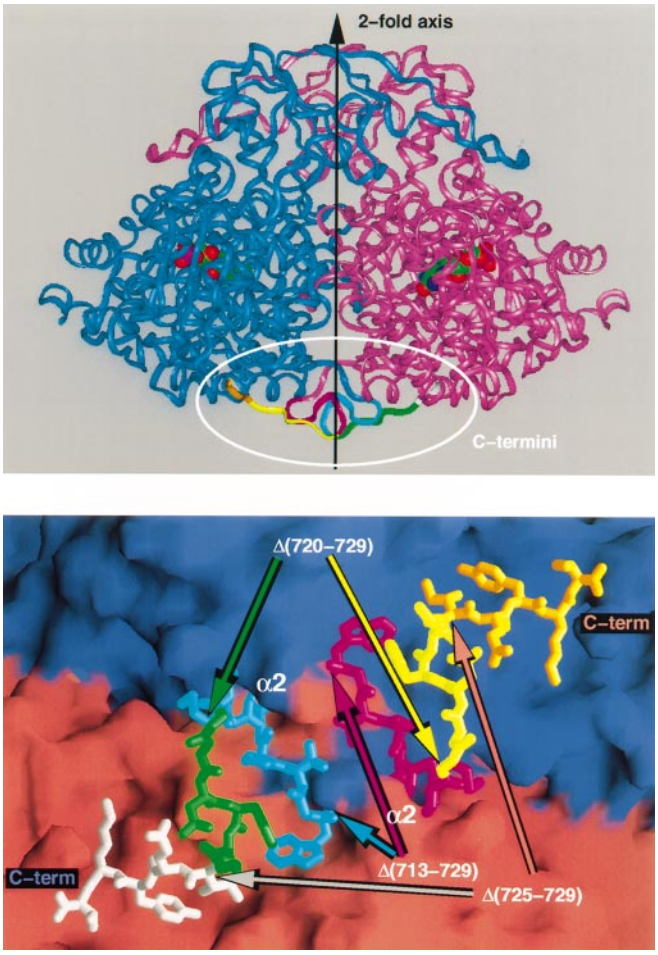

Fig. 1. Structure of trimethylamine dehydrogenase. (**Top**) Ribbon representation of the homodimer indicating the position of the 17 C-terminal residues in the structure. The FMN is shown in CPK. (**Bottom**) Close up view, showing the positions of the C-terminal deletions. The surfaces of two subunits, minus the last 17 amino acids, are coloured salmon and lilac. The C-terminal residues associated with the salmon subunit are coloured pink (713–719), yellow (720–724) and straw (725–729); those associated with the lilac subunit are coloured cyan (713–719), green (720–724) and white (725–729). The points at which the C-terminal deletions occur are denoted by the respective arrows, and the point where the C-terminal residues come into contact with the second α-helix of the β/α barrel of the same subunit is denoted 'α2'. The two C-termini are labelled in the colour of the subunit to which they belong.

Structure analysis

The 1.8 Å crystal structure (F.S.Mathews and S.A.White, unpublished results; Brookhaven code 2TMD) was analysed using interactive molecular graphics (InsightII; Molecular Simulations Inc., San Diego, USA). Solvent accessibility calculations were performed using the program XPLOR 3.843 (Brünger, 1996), with a probe radius of 1.4 Å.

Results

C-terminal deletions in relation to the structure of TMADH

The position of the C-terminal deletions in TMADH is shown in Figure 1. Inspection of the crystal structure reveals that residues in the N-terminal part of the second α-helix in the β/α barrel (particularly Glu80, Gly81 and Arg84) are in contact with residues His717, Met718 and Pro719 [deleted in mutant Δ(713–729)]. The C-terminal residues in each subunit are related by twofold symmetry and each extension embraces

Table I. Kinetic parameters and cofactor stoichiometries for native and recombinant trimethylamine dehydrogenases

Enzyme	K_m (μM)	k_{cat} (s^{-1})	ADP (mol/mol enzyme)	Iron (mol/mol) enzyme	Flavin (%)
Native WT	13.7 ± 1.7	15.6 ± 2.4	1.2	4.5	96
Recomb. WT	9.6 ± 1.5	10.2 ± 2.0	1.3	4.1	24
Δ(725–729)	4.6 ± 1	5.6 ± 0.3	1.5	5.8	2.4
Δ(720–729)	4.7 ± 2	6.4 ± 0.5	1.5	3.9	0.8
Δ(713–729)	n.d.	n.d.	1.1	4.4	0.4

Flavinylation levels were calculated from fluorescence data assuming native enzyme is 96% flavinylated (Packman *et al*., 1995). Kinetic parameters were calculated by fitting data to the steady state rate equation described by Falzon and Davidson (1996a), which takes account of inhibition at high substrate concentrations. Values of k_{cat} were determined based on flavinylated protein rather than total protein. n.d. not determined, since levels of activity were too low for a steady-state analysis. Low levels of activity were seen for the purified Δ(713–729) enzyme (0.3% the activity of the native wild-type enzyme under standard assay conditions; see Materials and Methods). The low level of activity for the Δ(713–729) mutant prevented more detailed analysis in steady-state assays.

the non-orginating subunit. On deletion of C-terminal residues in the Δ(725–729), Δ(720–729) and Δ(713–729) mutants, the change in exposed hydrophobic surface area was calculated (based on the wild-type crystal structure and in the absence of any conformational change in structure). Expressed relative to the wild-type enzyme, these changes are +70 $Å^2$ [Δ(725–729)], –74 $Å^2$ [Δ(720–729)] and –374 $Å^2$ [Δ(713–729)], respectively.

General properties of the mutant enzymes

Mutant enzymes were constructed and purified to homogeneity as described. During the purification procedure, only low levels of activity were detected for each of the mutant enzymes and in the pure form the activities of all three mutants were found to be substantially reduced compared with native wild-type and recombinant wild-type enzymes (Table I). The difference in specific activity of native and recombinant wild-type enzymes was previously shown to be a result of under-flavinylation of the recombinant enzyme (Scrutton *et al*., 1994; Packman *et al*., 1995; Mewies *et al*., 1996). Recombinant wild-type and mutant forms of TMADH in which residues critical to the flavinylation chemistry have not been targeted are consistently isolated with 25 to 35% of the enzyme in the flavinylated form (e.g. see Scrutton *et al*., 1994; Wilson *et al*., 1997a). For the C-terminal deletion mutants of TMADH, it was necessary to establish, therefore, whether the low specific activities of the mutants were due to poor flavinylation (<<25%) of the enzyme or some other major structural alteration in the active site.

The UV-visible absorption spectra of the three mutant enzymes were found to be markedly different from those of the native and recombinant wild-type proteins (Figure 2). The decreased absorbance at 443 nm and the shift in peak position toward lower wavelength is suggestive of poor flavinylation of the mutant enzymes, whilst the broad absorption between 330 nm and 550 nm suggests that the 4Fe–4S centre is retained. Indeed, the spectrum of the Δ(713–729) mutant is remarkably similar to the spectra recorded for mutant forms of TMADH that are devoid of FMN in the active site due to the mutation of residues known to be involved in flavinylation chemistry (Mewies *et al*., 1996). The small increase in absorption at around 440 nm for the Δ(720–729) and Δ(725–729) mutants

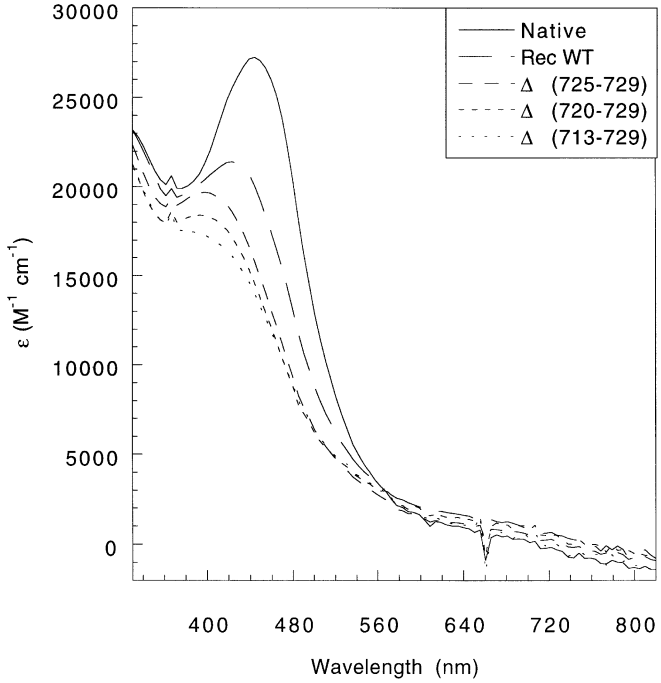

Fig. 2. Absorption spectra of native and recombinant forms of trimethylamine dehydrogenase. Molar absorption coefficients refer to a single active site. Spectra were recorded for enzyme samples dissolved in 0.1 M potassium phosphate buffer, pH 7.5. Rec WT, recombinant wild-type.

suggests that these enzymes contain small amounts of flavin in the active site.

The inferences made from the UV-visible absorption data were corroborated by cofactor analysis of clarified supernatants following precipitation of enzyme samples with perchloric acid. Analysis for released iron and ADP indicated that the 4Fe–4S centres and ADP are stoichiometrically assembled with each of the mutant proteins (Table I), thereby indicating that the observed spectral differences for the mutant enzymes are related to changes in flavin content. Fluorescence methods (Mewies *et al*., 1996) were employed to analyse flavin released into the supernatants and flavin linked to the precipitated enzyme via the 6-*S*-cysteinyl linkage, following acid precipitation of the various forms of TMADH. Flavin was not detected in the supernatants of the mutant enzymes, but small quantities of flavin were found associated with the precipitated protein. The degree of flavinylation is small; the level for the Δ(725–729) mutant is similar to levels determined previously for selected active site mutants of TMADH in which residues involved in the flavinylation mechanism were targeted (Packman *et al*., 1995; Mewies *et al*., 1996). The levels determined for the Δ(720–729) and Δ(713–729) are significant, but the lowest seen to date for any recombinant form of TMADH. The small amount of flavin found in each of the three mutant enzymes is consistent with the low levels of enzyme activity. The data indicate that each of the C-terminal deletion mutants is able to catalyse the formation of the 6-*S*-cysteinyl FMN, but that the efficiency of this reaction is severely compromised compared with the native and recombinant wild-type proteins. Clearly, the deletion of the C-terminal region of TMADH has long-range effects on the flavinylation reaction catalysed by the enzyme in the N-terminal β/α barrel domain. The small fraction of enzyme molecules that are flavinylated, however, are able to demethylate trimethylamine in the active site as

readily as the wild-type enzyme (Table I), suggesting that the C-terminal deletion mutants have an active site structure similar, if not identical, to wild-type. Consequently, the long-range effects on flavinylation in the active site most probably occur during folding and assembly of the enzyme with FMN; following the attainment of the fully folded and flavinylated mutant enzymes, the active site structure is sufficiently 'native-like' to efficiently catalyse the demethylation of trimethylamine.

Analysis of solution structure by circular dichroism spectroscopy

Near-UV and far-UV circular dichroism spectroscopy was performed to gain insight into differences in the solution structure of each of the three mutant enzymes (<2.4% flavinylated) compared with the recombinant (24% flavinylated) and native (96% flavinylated) wild-type enzymes. In the far-UV region (205–240 nm), the spectrum of each mutant was essentially identical to the spectrum of native and recombinant TMADH. The data indicate that no major structural changes have occurred either as a result of deleting up to 17 residues from the C-terminus of the enzyme or as a consequence of underflavinylation of the recombinant wild-type or mutant forms of TMADH (Figure 3). Differences in CD spectra were observed below about 205 nm; the molecular ellipticity of the Δ(713–729) ~ Δ(720–729) > Δ(725–729) >> recombinant wild-type > native wild-type. These changes in CD signal are not due to major changes in protein structure (since the spectrum of each enzyme is identical in the range 205–240 nm) and are most likely due to the different flavin occupancies in the active sites of the enzymes.

The flavinylation levels of the recombinant enzymes also affect the CD spectra recorded in the near-UV region (Figure 3). The isoalloxazine ring of the 6-*S*-cysteinyl FMN of TMADH is located in a region of the active site that is rich in aromatic residues. For example, Trp355, Trp264 and Tyr60 provide binding determinants for the cationic substrate trimethylammonium (Lim *et al*., 1986; Bellamy *et al*., 1989). Additionally, Tyr169 is located close to the dihydrouracil portion of the isoalloxazine ring. It is likely that the absence of FMN in the active site will induce local structural changes in this region of the protein. A comparison of the near-UV CD data for native and recombinant wild-type indicates that underflavinylation markedly affects the aromatic region of the spectrum. These spectral changes are, in the main, most likely attributable to local adjustments in the positioning of the aromatic residues in the active site. The most striking difference occurs at about 290 nm, i.e. the peak is enhanced as flavin content is raised. A single tryptophan residue (Trp713) is removed in the Δ(713–729) mutant, but retained in the Δ(720–729) and Δ(725–729) enzymes. The near-UV CD spectra of the three deletion mutants are almost identical [with only a small reduction in molecular ellipticity at 250–260 nm for the Δ(713–729) mutant] indicating that the major changes between native and recombinant enzymes at 290 nm are related to flavin content.

Values of $g(s^*)_{max}$ for wild-type TMADH and mutants Δ(713–729), Δ(720–729) and Δ(725–729)

The computation of the value $g(s^*)_{max}$, rather than the more traditional estimation from boundary migration, enables a very high level of precision to be attained in measured sedimentation coefficients. This is chiefly because, provided that the distribution of $g(s^*)$ in s is clearly Gaussian and

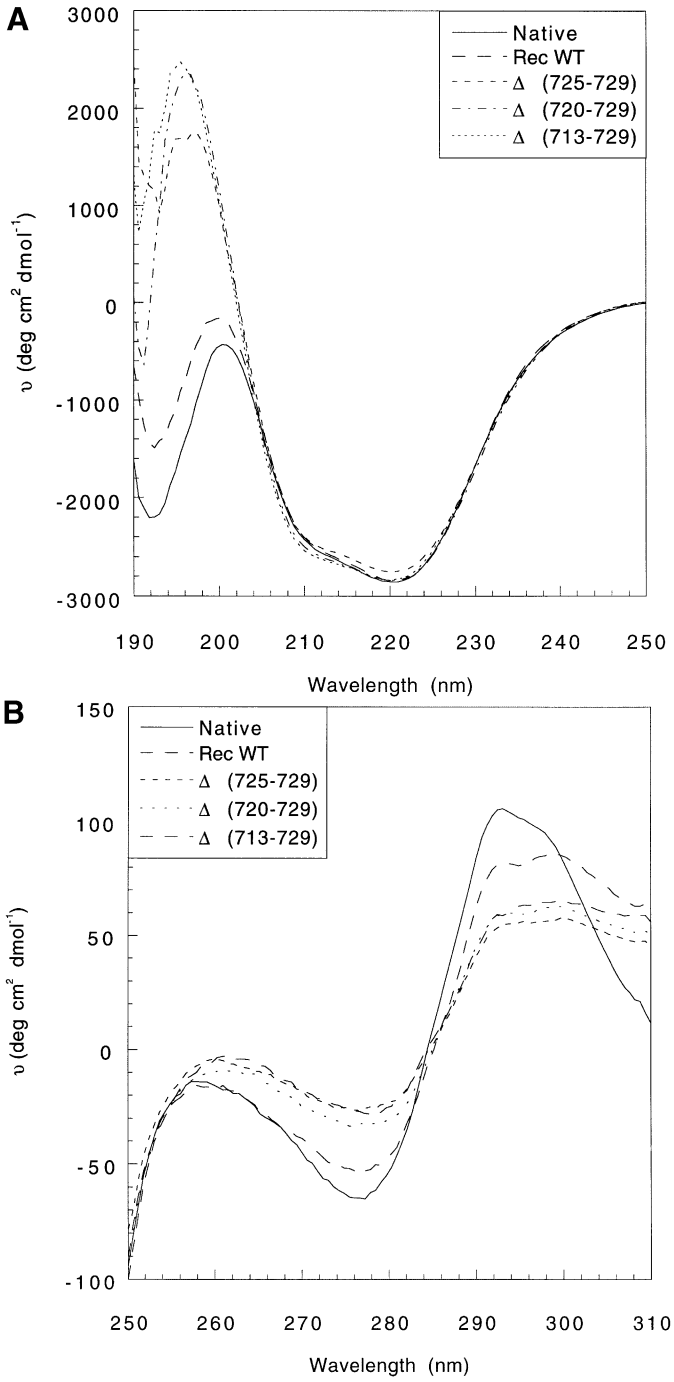

Fig. 3. Far-UV and near-UV spectra of native and recombinant trimethylamine dehydrogenases. (**A**) Far-UV CD spectra. (**B**) Near-UV CD spectra. Spectra were recorded for enzyme samples dissolved in 50 mM potassium phosphate buffer, pH 7.5. Rec WT, recombinant wild-type.

unimodal, then much more efficient use is made of the data of dn/dr versus r, which is now, using the AUC Imager, automatically logged from schlieren patterns. The precision attainable was tested by means of runs in which all three channels were allocated to identical solutions of the native wild-type protein, and estimated as ±0.005 S. As 'run on run' precision is inevitably worse than this, due to velocity and temperature uncertainties, all data for the mutants were normalized against a consensus value (9.092 S; Table II) of $g(s^*)_{max}$ for the native wild-type.

Patterns for all of these samples showed a clearly unimodal

Table II. Values of $g(s^*)_{max}$ for the wild-type and mutant forms of TMADH

Enzyme	$g(s^*)_{max}$ value	Predicted $g(s^*)_{max}$ value	$\Delta g(s^*)_{max}$[a]
Native WT	9.092 ± 0.006	–	–
Recomb. WT	8.677 ± 0.004	–	–
Δ(725–729)	8.726 ± 0.005	8.633	+0.098
Δ(720–729)	8.707 ± 0.006	8.597	+0.110
Δ(713–729)	8.795 ± 0.005	8.540	+0.255

The values of $g(s^*)_{max}$ predicted for the three deletion mutants of TMADH are compared with the values expected solely on the basis of the loss of mass as compared with wild-type (assuming $s \propto M^{2/3}$ for no change in gross conformation or in solvation). No allowance has been made for the effect of the lower degree of flavinylation of the three C-terminal constructs—such an effect would be very small, and would slightly increase the magnitude of the changes observed.

[a]Changes in $g(s^*)_{max}$ with respect to recombinant wild-type are given. The algebraic sign shows that the structures are more compact than would be expected simply by deleting the appropriate residues.

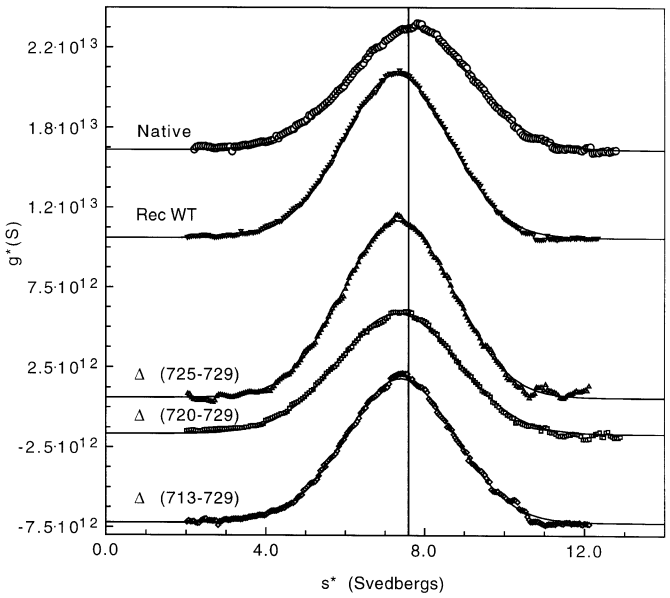

Fig. 4. Plots of $g(s^*)$ versus s (sedimentation coefficient) for the wild-type and recombinant forms of TMADH. Vertical axes are displaced for clarity. The vertical line at 9.092 S is the value estimated for $g(s^*)_{max}$ for the native wild-type enzyme.

and accurately Gaussian distribution, confirming both the precision of the optical alignment and the monodispersity of the samples (Figure 4). Values for $g(s^*)_{max}$ for the three mutant samples are given in Table II, and compared with values 'corrected', relative to recombinant wild-type, for the lower mass of the three constructs having C-terminal deletions. The precision attained in $g(s^*)_{max}$ with all the mutants is very satisfactory. It is arguable that the quality of fit to a single Gaussian is slightly less good than for the wild-type, but this effect if present is of borderline statistical significance. There are small but clearly significant changes in the $g(s^*)_{max}$ value of all three mutant enzymes as compared with recombinant wild-type, even after allowance has been made for the lower total mass (Table II). The Δ(725–729) construct shows an increase in value, the Δ(720–729) only a very small further increase, whilst the Δ(713–729) construct shows an appreciable further increase. In all cases the changes seen are much larger

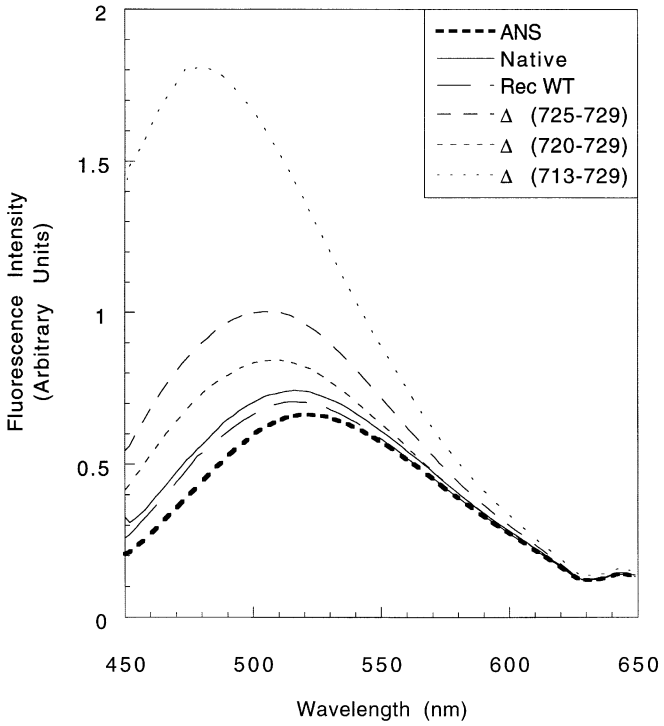

Fig. 5. Fluorescence spectra of free ANS and ANS in the presence of native and recombinant trimethylamine dehydrogenases. ANS (25 μM) and protein (0.1 mg/ml) solutions were prepared in 50 mM potassium phosphate buffer, pH 7.5.

than the available precision (Table II). The significance of these changes is discussed below.

Solution properties and stabilities of wild-type and mutants Δ(713–729), Δ(720–729) and Δ(725–729)

ANS binding was used as a sensitive method of analysing hydrophobic exposure in the wild-type and mutant TMADH enzymes. Emission spectra of free ANS and ANS in the presence of native and recombinant wild-type, and the three deletion mutants, were recorded following excitation at 365 nm. Native and recombinant wild-type enzymes show the same emission spectrum, again confirming that under-flavinylation of the wild-type enzyme does not lead to major structural change (Figure 5). Enhancement in ANS fluorescence (accompanied by a shift to shorter wavelength) is observed for each of the mutant proteins, with the largest increase in fluorescence seen for the Δ(713–729) mutant. These observations were compared with the expected change in exposed hydrophobic surface area, based on the 1.8 Å wild-type crystal structure, of the Δ(713–729), Δ(720–729) and Δ(725–729) mutants. An increase with respect to wild-type of 70 $Å^2$ was calculated for the Δ(725–729) mutant, consistent with the trend in ANS fluorescence. However, a decrease with respect to wild-type of 74 and 374 $Å^2$ was calculated for the Δ(720–729) and Δ(713–729) mutants, repectively. This is inconsistent with the trend in ANS fluorescence, and therefore suggests that conformational changes must accompany the deletion of residues at the C-terminus of TMADH to alter the degree of hydrophobic exposure.

Fluorescence emission following excitation at 295 nm as a function of guanidine hydrochloride concentration was used to probe the structural stabilities of the wild-type and mutant enzymes. Enzyme samples were incubated at room temperature for 30 min prior to fluorescence measurements; incubation

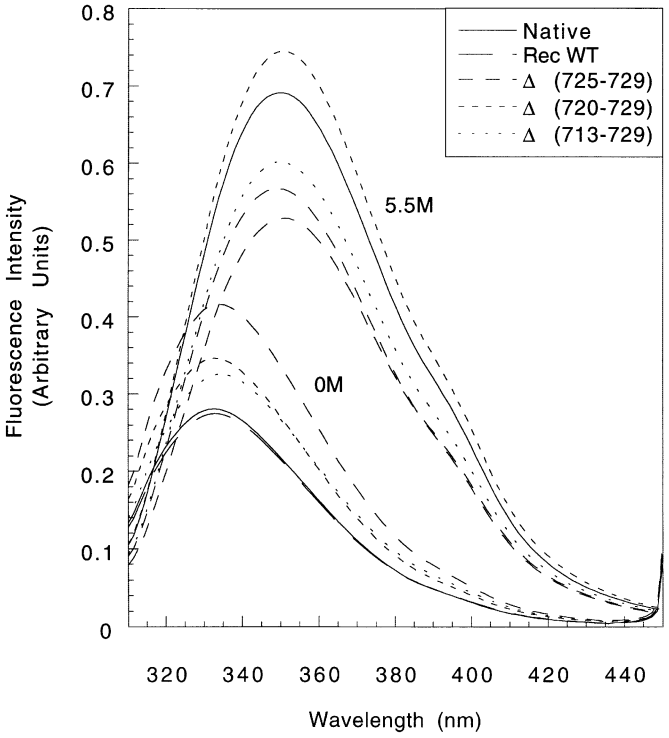

Fig. 6. Fluorescence emission spectra of native and recombinant trimethylamine dehydrogenases in the absence and presence of 5.5 M guanidine hydrochloride.

for extended periods of time (i.e. 60 and 180 min) did not lead to further changes in fluorescence emission. At an excitation wavelength of 295 nm, at which tryptophans are selectively excited, the emission maxima occurs at 355 nm (Figure 6). When normalized to the same protein concentration, the fluorescence quantum yield of each enzyme in the absence of denaturant is comparable. Full enhancement of fluorescence is achieved in the presence of 5.5 M guanidine hydrochloride and is accompanied by a shift in peak maxima to about 350 nm. The three mutant enzymes exhibit similar increases in fluorescence intensity [1.76-, 1.71- and 1.60-fold for the Δ(725–729), Δ(720–729) and Δ(713–729) enzymes, respectively] on the addition of denaturant, whereas larger increases were observed for the native (2.43-fold) and recombinant wild-type (2.0-fold) enzymes. These differences in fluorescence intensity are most likely related to flavin content since the intensity changes on moving from the folded to the unfolded states are larger for those enzymes with a higher content of 6-*S*-cysteinyl FMN.

The enhancement in total fluorescence intensity as a function of denaturant for the wild-type and recombinant wild-type enzymes occurs over the range 1–2 M guanidine hydrochloride and these data indicate that partial flavinylation in the recombinant wild-type does not compromise the stability of the enzyme dimer (Figure 7). The unfolding curves are irreversible (thereby preventing the calculation of free energy changes of unfolding) and are accompanied by loss of the 4Fe–4S centre and ADP. The unfolding transitions of the Δ(713–729) and Δ(720–729) are coincident and are broader (<0.5 to 2 M) than those seen for the wild-type enzymes (1–2 M). Full fluorescence intensity for these mutants is obtained at the same denaturant concentration as the wild-type enzymes, but unfolding begins at lower concentrations. The

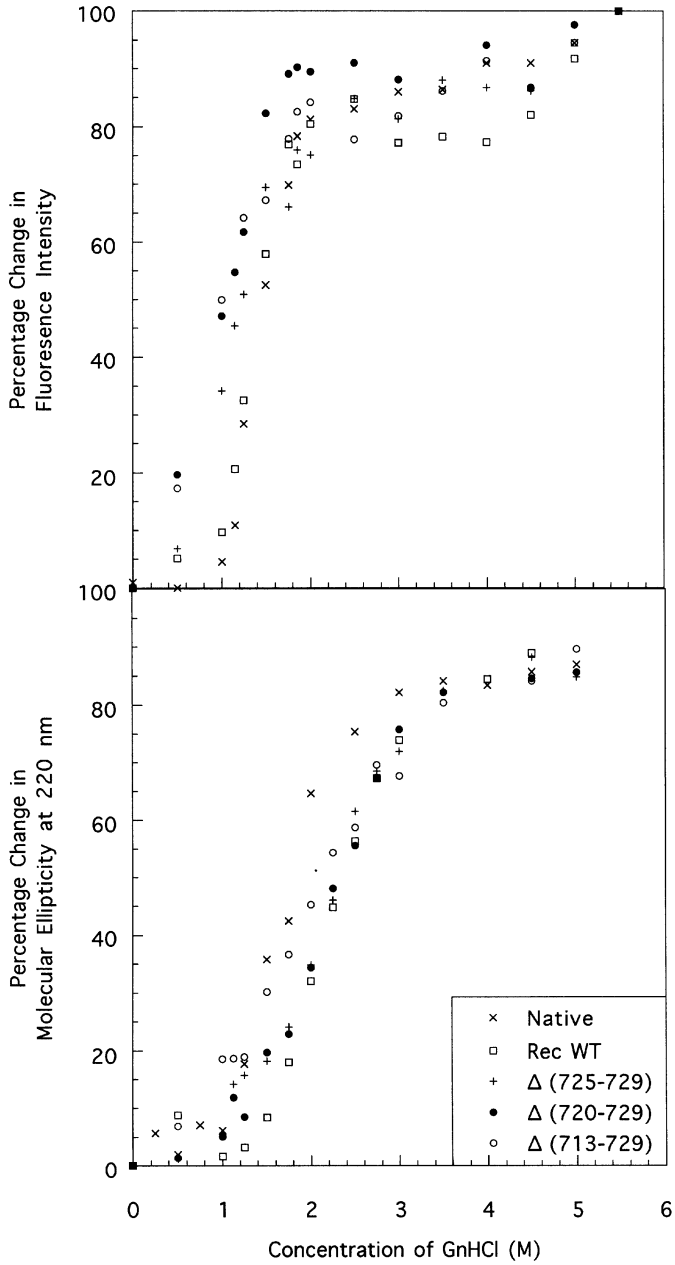

Fig. 7. Guanidine-induced unfolding of native and recombinant trimethylamine dehydrogenases monitored by enhanced fluorescence emission and circular dichroism spectroscopy.

broader transition for the Δ(713–729) and Δ(720–729) mutant proteins indicates partial unfolding occurs at lower denaturant concentrations. Initial unfolding of the Δ(725–729) occurs at denaturant concentrations intermediate of those for the wild-type enzymes and the Δ(713–729) and Δ(720–729) mutant enzymes, but again the fluorescence transition is complete at 2 M denaturant as seen for all the enzymes. Similar results were obtained when the maximum emission wavelength was plotted against denaturant concentration (data not shown).

Guanidine-induced denaturation of the mutant and wild-type enzymes was also monitored by circular dichroism spectroscopy by monitoring ellipticity changes at 222 nm (Figure 7). In contrast to the fluorescence data, the unfolding transitions of the wild-type and mutant enzymes were approximately coincident and the transitions occurred over a denaturant

range of 1–3 M. Enhancement in fluorescence intensity at low guanidine concentrations for the deletion mutants does not, therefore, correspond with a significant loss in overall structure, and full enhancement in fluorescence intensity at 2 M guanidine is achieved before complete unfolding at 3 M guanidine as measured by circular dichroism spectroscopy. That fluorescence intensity for the deletion mutants is enhanced before significant loss of structure again suggests a local loosening of structure (perhaps in the region of the C-terminal deletions) at low concentrations of denaturant.

Discussion

In this paper, the conformational states and solution properties of recombinant TMADH enzymes deleted in the C-terminal region have been investigated. The high resolution crystallographic structure of TMADH reveals that residues 713–729 of each subunit wrap around surface residues on the other subunit (Figure 1), suggesting a role for these residues in either (i) conferring stability on the assembled homodimer or (ii) guiding subunit–subunit association during assembly of the enzyme. Contrary to the first suggestion, we have found that deletion of the C-terminal residues in mutants Δ(725–729), Δ(720–729) and Δ(713–729) does not compromise significantly dimer stability (as indicated by the formation of dimeric TMADH and circular dichroism studies of guanidine-induced unfolding of the enzymes), but adversely effects flavinylation of the enzyme at the active site some 20 Å from the point of mutation. Only a small portion of the purified mutant enzymes are assembled with 6-*S*-cysteinyl FMN; the kinetic behaviours of the flavinylated proteins [with the possible exception of the Δ(713–729), for which steady-state data was not collected due to the very low flavin content of the enzyme] are similar to the native and recombinant wild-type enzymes, implying that there are no significant structural differences in the active sites of the flavinylated mutant enzymes. The substantial reduction in the degree of flavinylation for the mutant enzymes suggests that the C-terminal deletions affect protein folding and thereby assembly with FMN, since it is thought that FMN binds to TMADH before fully folded enzyme is attained (Packman *et al*., 1995; Mewies *et al*., 1996). Other than flavin content, the differences in molecular structure between the flavinylated and deflavo forms of the mutant TMADH enzymes are minor. Since the flavinylated forms retain full catalytic activity, they must be assembled with flavin, the 4Fe–4S centre and presumably ADP (which has no known catalytic function); the very low quantities of the flavinylated forms of the mutant enzymes did not allow direct chemical analysis for these cofactors. Chemical analysis indicated that the deflavo forms of the mutant proteins are fully assembled with the 4Fe–4S centre and ADP. In this regard, the findings are consistent with previous work on the deflavo form of recombinant wild-type TMADH (Scrutton *et al*., 1994). The CD spectra of the mutant proteins are very similar to those of the native and recombinant wild-type enzymes and the observed differences in the near- and far-UV regions can be attributed to affects directly related to flavin occupancy. Again, the data serve to reinforce the assertion that the deflavo forms of the mutant enzymes are overall structurally very similar to the wild-type enzymes.

Minor differences between the deflavo C-terminal deletion mutants, the recombinant wild-type (24% flavinylated) and native (96% flavinylated) enzymes are seen in ANS binding studies and fluorescence enhancement during guandine-induced unfolding. The latter experiments indicate a broader transition in unfolding for the deletion mutants, suggesting a local 'loosening' of structure at low guanidine concentration compared with the wild-type enzymes. This 'loosening' in structure is most likely associated with that part of the molecule close to the C-terminal deletions. Differences in fluorescence emission during ANS binding and the calculated changes in hydrophobic exposure based on the wild-type crystallographic structure suggest there are conformational changes associated with the C-terminal deletions. Since ANS binding is not affected by the degree of flavin occupancy in the active site (compare fluorescence emission for native and recombinant wild-type enzymes; Table II), the predicted conformational change is likely to be local to the C-terminal regions.

Further evidence for conformational changes on deleting residues at the C-terminus of TMADH was gained from hydrodynamic studies of the wild-type and mutant proteins. The hydrodynamic studies, in which there is a small decrease (not detectable using other physical solution methods) in translational friction as measured by the change in $g(s^*)_{max}$ with respect to recombinant wild-type in all three deletions, suggest that the structure becomes more compact when C-terminal deletions are made. This increase in compactness is significantly larger than that expected from the loss of mass for the deletions alone, implying a conformational change. We believe this is the first time that the precise, unapproximated distributions of $g(s^*)$, which can be computed directly from schlieren patterns (i.e. derivative data) via the Bridgman equation, have been put to practical use. Unlike the time derivative method (Stafford, 1992), there are no approximations made involving the diffusion coefficients of the species under study. This is particulary important where very small changes in molecular structure, of the type reported in this paper, are being investigated. The hydrodynamic studies have not only served to reveal the rather subtle changes in conformation on deleting the C-terminal residues in TMADH, but they have also demonstrated that fully flavinylated wild-type enzyme is, as expected, more compact than recombinant wild-type, which is predominantly (76%) deflavo. Our data is consistent with studies on other flavoenzymes in which a more flexible structure is observed for deflavo enzyme giving rise, for example, to increased susceptibility to proteolysis (Tarelli *et al*., 1990) or increased temperature factors for crystalline forms in the absence of flavin (Schulz and Ermler, 1990).

The observed small changes in conformation for the C-terminal deletion mutants of TMADH can be rationalized as follows. In the crystallographic structure of wild-type TMADH, residues His717, Met718 and Pro719 [deleted in the Δ(713–729) mutant, see Figure 1] are found to interact with the N-terminal end of the second α-helix in the β/α barrel. Therefore, in the Δ(713–729) mutant, the β/α barrel domain could move further across towards the other subunit, thereby making the structure more compact. The Δ(720–729) and Δ(725–729) mutants could affect the intersubunit interface similarly, but to a smaller degree. This possibility is reflected in the increase in compactness with respect to recombinant wild-type of Δ(725–729) and Δ(720–729), and particularly Δ(713–729), shown in Table II. Since the active site lies within the β/α barrel domain, such a movement could leave the active site essentially unperturbed if the β/α barrel domain moved as a rigid body. Although the structural readjustments are not sufficently large to perturb the kinetic behaviour of the flavinylated portion of the C-terminal deletion mutant enzyme preparations, the conformational changes are sufficient to

severely compromise flavinylation with FMN during the assembly of TMADH. The conformational differences observed in the mutant enzymes are likely also to reflect minor structural differences during folding and assembly of TMADH. Underflavinylation of the mutant proteins is most likely related to the folding process, since fully folded deflavo TMADH cannot be reconstituted with FMN (Scrutton *et al*., 1994), which in turn is likely due to a crystallographically observed inorganic anion occupying the binding site of the phosphate moiety of FMN in the deflavo enzyme (Mathews *et al*., 1996). The observed effects on flavinylation brought about by the C-terminal mutations serve to illustrate the importance of subtle and long-range protein–protein interactions during the molecular assembly of TMADH.

Acknowledgements

This work was funded by the Royal Society (N.S.S. and M.J.S.), the Biotechnology and Biological Sciences Research Council (N.S.S.) and Leicester University (S.R.). We thank Mr B.Pope (MRC Laboratory of Molecular Biology, Cambridge) for assistance with circular dichroism measurements.

References

Basran,J., Mewies,M., Mathews,F.S. and Scrutton,N.S. (1997) *Biochemistry*, **36**, 1989–1998.

Bellamy,H.D., Lim,L.W., Mathews,F.S. and Dunham,W.R. (1989) *J. Biol. Chem.*, **264**, 11887–11892.

Boyd,G., Mathews,F.S., Packman,L.C. and Scrutton,N.S. (1992) *FEBS Lett.*, **308**, 271–276.

Bradford,M. (1976) *Anal. Biochem.*, **72**, 248–254.

Bridgman,W.B. (1942) *J. Am. Chem. Soc.*, **64**, 2349–2350.

Brünger,A.T. *XPLOR* Manual Version 3.843. Yale University, 1996.

Clelow,A.C., Errington,N. and Rowe,A.J. (1997) *Eur. Biophys. J.*, **25**, 311–317.

Cölfen,H., Harding,S.E., Wilson,E.K., Packman,L.C. and Scrutton,N.S. (1996) *Eur. Biophys. J.*, **24**, 159–164.

Falzon,L. and Davidson,V.L. (1996a) *Biochemistry*, **35**, 2445–2452.

Falzon,L. and Davidson,V.L. (1996b) *Biochemistry*, **35**, 12111–12118.

Hill,C.L., Steenkamp,D. J., Holm,R.H. and Singer,T.P. (1977) *Proc. Natl Acad. Sci. USA*, **74**, 547–551.

Huang,L., Rohlfs,R.J. and Hille,R. (1995) *J. Biol. Chem.*, **270**, 23958–23965.

Kasprazak,A.A., Papas,E.J. and Steenkamp,D.J. (1983) *Biochem. J.*, **211**, 535–541.

Kenney,W.C., McIntire,W., Steenkamp,D.J. and Benisek,W.F. (1978) *FEBS Lett.*, **85**, 137–139.

Laemmli,U.K. (1974) *Nature*, **227**, 680–685.

Lim,L.W., Shamala,N., Mathews,F.S., Steenkamp,D.J., Hamlin,R. and Xuong,N. (1986) *J. Biol. Chem.*, **261**, 15140–15146.

Lim,L.W., Mathews,F.S. and Steenkamp,D.J. (1988) *J. Biol. Chem.*, **263**, 3075–3078.

Lloyd,P.H. (1974) In *Optical Methods in Ultracentrifugation, Electrophoresis and Diffusion* (Monographs on Physical Biochemistry series). Clarendon Press, Oxford, Chapter 3, pp. 21–37.

Mathews,F.S., Trickey,P., Barton,J.D., Chen,Z.-W. and Scrutton,N.S. (1996) In Stevenson,K.J., Massey,V. and Williams,C.H. Jr. (eds) *Flavins and Flavoproteins.* University of Calgary Press, 873–876.

Mewies,M., Packman,L.C., Mathews,F.S. and Scrutton,N.S. (1996) *Biochem. J.*, **317**, 267–272.

Packman,L.C., Mewies,M. and Scrutton,N.S. (1995) *J. Biol. Chem.*, **270**, 13186–13191.

Rohlfs,R.J. and Hille,R. (1991) *J. Biol. Chem.*, **266**, 15244–15252.

Rohlfs,R.J. and Hille,R. (1994) *J. Biol. Chem.*, **269**, 30869–30879.

Rohlfs,R.J., Huang,L.X. and Hille,R. (1995) *J. Biol. Chem.*, **270**, 22196–22207.

Sambrook,J., Fritsch,E.F. and Maniatis,T. (1989) *Molecular Cloning: A Laboratory Manual*, 2nd Edn. Cold Spring Harbor Laboratory Press, Cold Spring Harbor, NY.

Schulz,G.E. and Ermler,U. (1990) In Curti,B., Ronchi,S. and Zanetti,G. (eds), *Flavins and Flavoproteins.* de Gruyter and Co., Berlin-New York, pp. 505–512.

Scrutton,N.S. (1994) *BioEssays*, **16**, 115–122.

Scrutton,N.S., Packman,L.C., Mathews,F.S., Rohlfs,R.J. and Hille,R. (1994) *J. Biol. Chem.*, **269**, 13942–13950.

Stafford,W.F. (1992) *Anal. Biochem.*, **203**, 295–301.

Steenkamp,D.J. and Gallup,M. (1978) *J. Biol. Chem.*, **253**, 4086–4089.

Steenkamp,D.J. and Mallinson,J. (1976) *Biochim. Biophys. Acta*, **429**, 705–719.

Steenkamp,D.J., McIntire,W. and Kenny,W.C. (1978a) *J. Biol. Chem.*, **253**, 2818–2824.

Steenkamp,D.J., Singer,T.P. and Beinert,H. (1978b) *Biochem J.*, **169**, 361–369.

Svensson,H. (1954) *Optica Acta.*, **1**, 25–32.

Tarelli,G.T., Vanoni,M.A. and Curti,B. (1990) In Curti,B., Ronchi,S. and Zanetti,G. (eds), *Flavins and Flavoproteins*. de Gruyter and Co., Berlin-New York, pp. 155–158.

Weber,G. and Young,L.B. (1964) *J. Biol. Chem.*, **239**, 1415–1423.

Wilson,E.K., Mathews,F.S., Packman,L.C. and Scrutton,N.S. (1995) *Biochemistry*, **34**, 2584–2591.

Wilson,E.K., Huang,L., Sutcliffe,M.J., Mathews,F.S., Hille,R. and Scrutton,N.S. (1997a) *Biochemistry*, **35**, 41–48.

Wilson,E.K., Scrutton,N.S., Cölfen,H., Harding,S.E., Jacobsen,M.P. and Winzor,D.J. (1997b) *Eur. J. Biochem.*, **243**, 393–399.

Received June 24, 1997; revised February 2, 1998; accepted February 12, 1998